LA-UR-15-20076
Approved for public release; distribution is unlimited.

Title: Hypothesis to Explain the Size Effect Observed in APO-BMI Compression Tests

Author(s): Schembri, Philip Edward
Siranosian, Antranik Antonio
Kingston, Lance Allen

Intended for: Internal distribution

Issued: 2015-01-07

Hypothesis to Explain the Size Effect Observed in APO-BMI Compression Tests

Philip Schembri, Antranik Siranosian, Lance Kingston

10/3/2014

In 2013 compression tests were performed on cylindrical specimens of carbon-microballoon-APO-BMI syntactic foam machined to different lengths (0.25, 0.5, and 2.8 inches[1]) (Kingston, 2013). In 2014 similar tests were performed on glass-microballoon-APO-BMI of different lengths (~0.15", ~0.32", and ~0.57"). In all these tests it was observed that, when strains were calculated from the platen displacement (corrected for machine compliance), the apparent Young's modulus of the material decreased with specimen size, as shown in Table 1. The reason for this size effect was speculated to be a layer of damage on or near the top and bottom machined surfaces of the specimens (Kingston, Schembri, & Siranosian, 2014). This report examines that hypothesis in further detail.

By approximating the assumed damaged and undamaged portions of the specimen as linear springs in series (see (Kingston, Schembri, & Siranosian, 2014)), the apparent specimen compliance can be decomposed into the sum of the compliance of the damaged and undamaged lengths of specimen:

$$C_{app}=C_d+C_u \tag{1}$$

where C_{app} is the apparent specimen compliance, C_d is the compliance of the damaged length, l_d, of the specimen, and C_u is the compliance of the undamaged length, l_u, of the specimen. In terms of the apparent, damaged, and undamaged Young's moduli, E_{app}, E_d, and E_u, respectively, the compliances are

$$C_{app}=l/AE_{app} \tag{2}$$

$$C_d=2l_d/AE_d \tag{3}$$

$$C_u=l_u/AE_u \tag{4}$$

where A is the cross-sectional area and

$$l=2l_d+l_u \tag{5}$$

[1] 0.75 inch specimens were also tested, but the data is suspect because the loads were cycled.

is the total specimen length. Note that the factor of 2 is necessary because there are two damaged lengths, one at each end of the specimen, each with length l_d. Combining equations (1), (4), and (5), we can express the apparent compliance as a linear function of specimen length:

$$C_{app} = \left(C_d - \frac{2l_d}{AE_u} \right) + \frac{1}{AE_u} l \tag{6}$$

Note that if the damaged and undamaged moduli are equal then the y-intercept term (in parentheses) vanishes and the apparent modulus must equal the damaged (and undamaged) modulus. Furthermore, equation 6 shows that the observed magnitude of the specimen size effect (i.e. the magnitude of the y-intercept) grows with damaged length and with the difference between damaged and undamaged moduli. Also note that if the apparent compliance, as measured from tests, is plotted as a function of specimen length, the undamaged modulus can be estimated from the slope of a best fit line (as presented in (Kingston, Schembri, & Siranosian, 2014)). Such a plot is shown in Figure 1.

The close proximity of the data to the line in Figure 1 shows that this simple model of a compression specimen with damaged ends does indeed fit the data reasonably well. The undamaged modulus estimated from this best fit line is 132 ksi, which compares favorably to the 137 ksi undamaged modulus measured using an extensometer, thus eliminating end effects, on a 2.8 inch long specimen. This evidence supports the hypothesis that the size effect is caused by a damaged layer near the surfaces; however, the actual nature and cause of the damage was unexplored.

To investigate the nature and cause of the damage, MST-7 provided micro computed tomography (CT) images of the machined surface of one of the carbon APO-BMI specimens. Figure 2 shows one of these images; this is a cross-section, so the free surface runs approximately horizontally near the top of the image. As equation (6) suggests, the significant magnitude of the effect of specimen length on apparent modulus must be due to a large l_d, a very compliant damaged region, or both. The only obvious damage consists of the apparently broken microballoons on the free surface; it is not possible to discern from this image any damage below the surface. Thus, the question to be investigated is whether this surface region of broken microballoons is compliant enough to explain the observed specimen size effect.

There are two important features of the free surface shown in Figure 1 which we consider. First, this surface, containing broken microballoons and APO-BMI binder, is very irregular, with feature sizes on the order of the size of the larger microballoons (~50 microns, or 2 mils). This irregularity must reduce the contact area between the specimen and the steel compression platen, which has a much lower surface roughness, estimated to be on the order of 0.04 mils (Corporation). Second, without constrained, unbroken, microballoons to provide stiffness, the

material at this surface must have a much lower stiffness than the bulk material, on the order of that of APO-BMI binder, which may be on the order of 1-10 ksi (Densmore, 2008, p. 26).

Using our estimate of 132 ksi for the undamaged modulus from Figure 1, and a value of 50 microns (2 mils) for l_d, equation (6), when evaluated for the 2.8 inch long specimen, results in a damaged modulus of 4 ksi, which is on the same order as that of APO-BMI (i.e., the binder only). Thus, we conclude that the damaged and irregular surface shown in Figure 2 is indeed capable of causing the specimen size effect observed in the APO-BMI compression tests.

It might be more correct to categorize this phenomenon as a surface effect rather than a damage effect. In fact, similar phenomena have been described as *surface contact* effects in various materials, including concrete (Elwell & Fu, 1995), Steel and Aluminum (Goerke & Willner, 2008), (Konowalski, 2009)), and soils (Kustov & Ruppeneit, 1985). In the case of APO-BMI, the effect is enhanced because the stiffest constituent of the material (i.e., the microballoons) is damaged at the surface.

Understanding of this phenomenon in terms of a damaged surface leads to a simple method of including the effect in ABAQUS finite element (FE) models that use APO-BMI syntactic foams. ABAQUS[2] provides a method of including 'softened' contact between two materials, with the option of a linear relationship between contact pressure, p, and overclosure, h, (Dassault Systèmes Simulia Corp, 2014, p. 37.1.2). A stiffness value, k, used by ABAQUS as a penalty parameter to enforce the contact constraint, effectively relates overclosure to pressure as follows

$$p=kh \tag{7}$$

If we take the overclosure to represent the change in thickness of the damaged surface layer, i.e. to represent Δl_d, then the stress-strain relationship (Hooke's law) for the damaged surface can be written as

$$p=E_d\varepsilon_d=E_d\frac{h}{l_d} \tag{8}$$

where p now represents the (compressive) stress in the damaged surface normal to the interface, and ε_d is the (compressive) strain in the damaged surface. Comparing (7) and (8), we identify k as

$$k=\frac{E_d}{l_d} \tag{9}$$

Use of this modeling technique is demonstrated using FE calculations of two of the carbon APO-BMI specimens: the 0.5 inch long specimen, and the 2.8 inch long specimen. Figure 3 shows

[2] The keyword for this functionality is *Surface Behavior, pressure-overclosure=LINEAR

the two axisymmetric half-symmetry models. The upper mesh represents the platen, modeled as linear-elastic steel with a modulus of 30 Msi and Poisson's ration of 0.3. The lower mesh is the carbon APO-BMI specimen, which has a modulus of 132 ksi (i.e., the undamaged modulus, as estimated from Figure 1) and a Poisson's ratio of 0.3, which may not be representative but should not affect the results. The penalty stiffness, k, in the **Surface Behavior* keyword was chosen, using equation (9) with E_d=4 ksi and l_d=0.002 inches, to be 2000 ksi/inch. A uniform pressure resulting in ~1 ksi of axial compressive stress in the specimen, similar to the maximum load in the tests, is applied to the top surface of the platen.

The results of these two models were examined in the same way the test results were examined: an apparent Young's modulus of the test specimens was calculated by dividing the applied stress in the specimen by the strain calculated as the ratio of crosshead displacement to initial specimen length. The resulting apparent moduli for the 2.8 inch and 0.5 inch specimen models was 128 ksi and 105 ksi, similar to those that were obtained experimentally. Of course, the modulus calculated based on the specimen deformation rather than the platen displacement was 132 ksi since this was a material input value.

Note that while this should not be considered a validation calculation, since the experimental results were used to calibrate these models, it does demonstrate that the effect can be accounted for in FE models using the existing capabilities of ABAQUS. Furthermore, as the similarity of the 0.25 inch and 0.5 inch carbon APO-BMI apparent moduli shows, this phenomenon has a limited range over which it can be modeled as linear. Additionally, we have only accounted for the effect of the damaged layer in the direction normal to the interface; there may also be a tangential effect, but there have been no measurements of this.

In summary, examination of CT images of the surface of APO-BMI syntactic foam specimens resulted in refinement and verification of the hypothesis that a damaged region of the specimens causes their length to affect their apparent Young's modulus. Furthermore, a simple way to account for this effect in FE models, using existing ABAQUS features, was demonstrated.

Table 1 Summary of apparent Young's modulus versus specimen length for the Carbon and Glass microballoon APO-BMI

Carbon microballoons

Specimen length (in)	Apparent modulus (ksi)
0.25	99
0.5	98
2.8	128

Glass microballoons

Specimen length (in)	Apparent modulus (ksi)
0.15	46
0.32	77
0.57	101

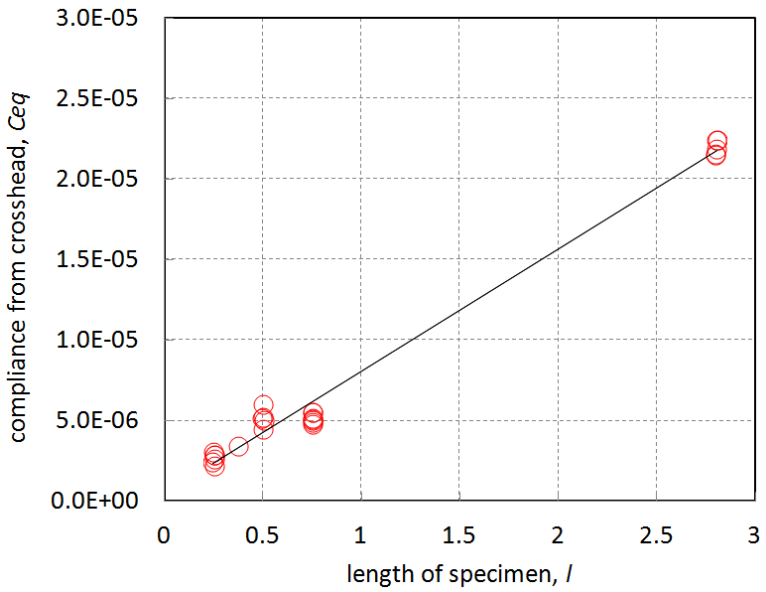

Figure 1. Best fit line through the experimentally collected carbon APO-BMI apparent moduli. The undamaged modulus estimated from the slope of this line is 132 ksi.

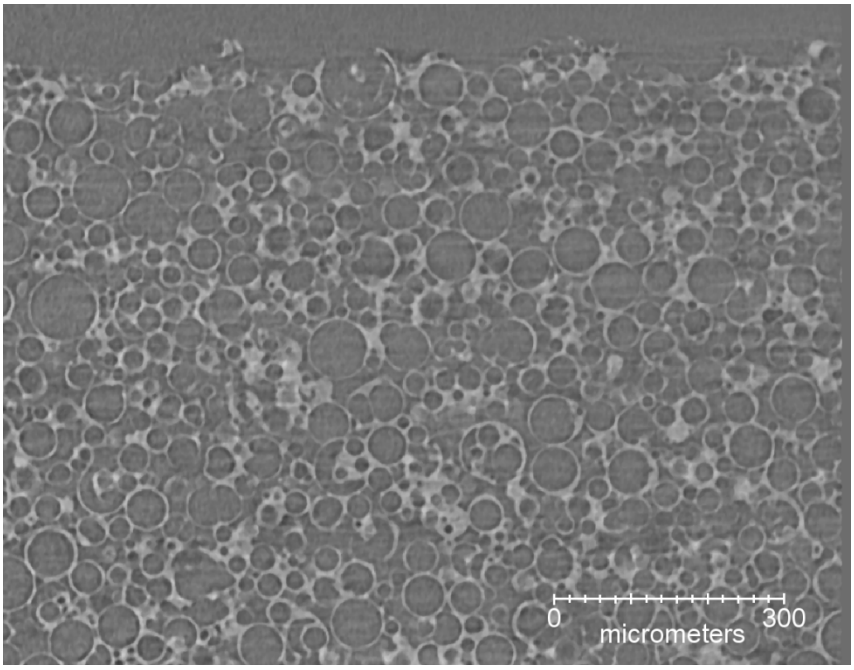

Figure 2 CT scan cross-section of a carbon-microballoon APO-BMI compression specimen showing the machined surface near the top of the image. Darker regions are regions of lower density. Image courtesy of Brian Patterson and Kevin Henderson, MST-7.

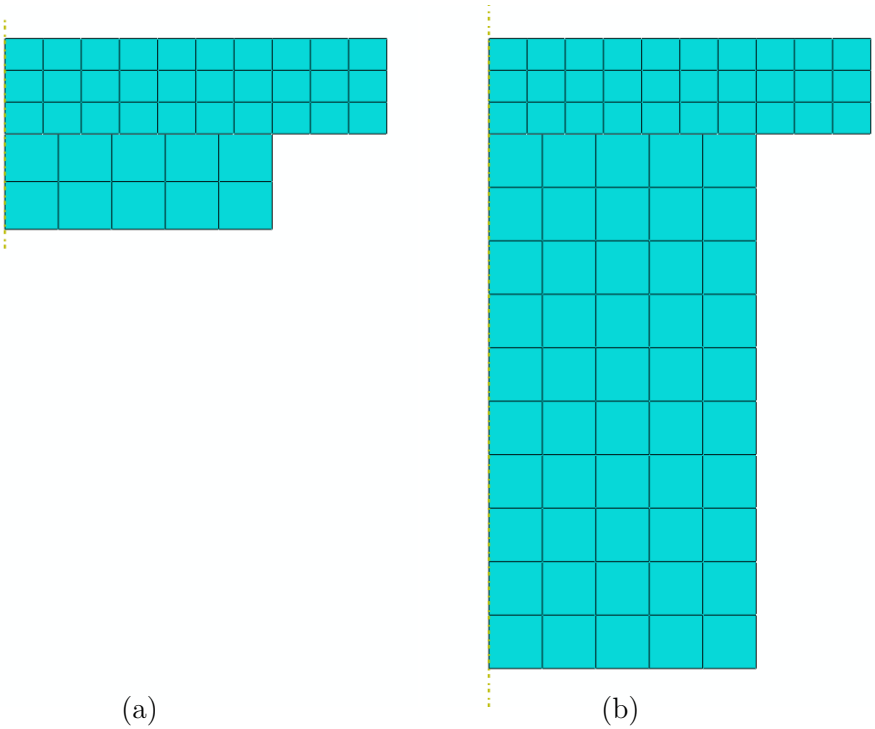

(a) (b)

Figure 3. Half-symmetry axisymmetric models of (a) the 0.5 inch long and (b) the 2.8 inch long carbon APO-BMI compression specimens and platen. A contact interaction with penalty stiffness equal to 2000 ksi/inch is defined on the edge where the two parts meet.

1 References

Corporation, U. S. (n.d.). *Surface Finish*. Retrieved October 2, 2014, from https://www.ussteel.com

Dassault Systèmes Simulia Corp. (2014). Abaqus Analysis User's Manual (V6.14), Section 37.1.2. Providence, RI, USA: Dassault Systèmes Simulia Corp.

Densmore, C. (2008). APO-BMI: A Historical Perspective and Recent Efforts Involving Production and Characterization, LA-UR-08-031682008.

Elwell, D. J., & Fu, G. (1995, March). Compression Testing of Concrete: Cylinders vs. Cubes. Transportation Research and Development Bureau.

Goerke, D., & Willner, K. (2008). Investigations of the influence of geometrical irregularities and roughness on the normal contact stiffness of joints. *Proc. Appl. Math. Mech. 8* , 10275 – 10276.

Kingston, L. (2013). *W-14-TR-0118: APO-BMI Foam Compression Test Report.* LANL.

Kingston, L., Schembri, P., & Siranosian, A. (2014, June). Measuring the Compressive Stiffness of Syntactic Foam Containing Carbon Microspheres, LA-UR-14-22597.

Konowalski, K. (2009). Experimental Research and Modeling of Normal Contact Stiffness and Contact Damping of Machined Joint Surfaces. *Advances in Manufacturing Science and Technology, 33(3)* , 53-68.

Kustov, V. V., & Ruppeneit, K. V. (1985). Soil deformation characteristics in compression tests. *Soil Mechanics and Foundation Engineering, 22(4)* , 155-161.